

Structures and Stabilities of CaO and MgO Clusters and Cluster Ions: An alternative interpretation of the experimental mass spectra.

Andrés Aguado* and José M. López

Departamento de Física Teórica, Universidad de Valladolid, Valladolid 47011, Spain

The structures and relative stabilities of doubly-charged nonstoichiometric $(\text{CaO})_n\text{Ca}^{2+}$ ($n=1-29$) cluster ions and of neutral stoichiometric $(\text{MgO})_n$ and $(\text{CaO})_n$ ($n=3,6,9,12,15,18$) clusters are studied through *ab initio* Perturbed Ion plus polarization calculations. The large coordination-dependent polarizabilities of oxide anions favor the formation of surface sites, making the critical cluster size where anions with bulk coordination first appear larger than that found in the related case of alkali halides. Thus, we show that there are substantial structural differences between alkali halide and alkaline-earth oxide cluster ions, contrary to what is suggested by the similarities in the experimental mass spectra. An alternative interpretation of the magic numbers for the case of oxides is proposed, which involves an explicit consideration of isomer structures different from the ground states. A comparison with the previously studied $(\text{MgO})_n\text{Mg}^{2+}$ cluster ions shows that the emergence of bulklike structural properties with size is slower for calcium oxide. Nevertheless, the structures of the doubly charged clusters are rather similar for the two materials. On the contrary, the study of the neutrals reveals interesting structural differences between MgO and CaO, similar to those found in the case of alkali halides.

PACS numbers: 36.40.c; 61.46.+w; 61.50.Lt; 61.60.+m; 79.60.Eq

I. INTRODUCTION

Small clusters are of great interest both to the physical and chemical communities because of their numerous potential applications (for example, in nanoelectronics or catalysis), and also because one can gain important insight into the evolution from atomic and molecular properties to bulk and surface properties. To have a knowledge of the structures adopted by the clusters is of paramount importance, as many interesting cluster properties are largely determined by them. From the theoretical side, finding the lowest energy structure for each cluster is a complicated matter, because the number of isomers increases exponentially with cluster size. Other reasons are that one has to treat bulklike and surfacelike ions on an equal footing, and that the number of ions to be explicitly considered in a cluster is larger than in a bulk or surface study, where symmetry restrictions impose a number of useful atomic equivalences. From the experimental side, the problem is so difficult that during the approximately 30 years of intensive cluster research, the main source of structural information has been theory. Very recently, experimental techniques like electron diffraction from trapped clusters¹ or measurements of cluster mobilities²⁻⁶ have been successfully applied to study the structures of covalent and ionic clusters. Photoelectron spectroscopy has also been applied to study isomerization transitions in small alkali halide clusters,⁷ and measurements of ionization potential to detect structural transitions in barium oxide clusters.⁸ At the moment, however, these techniques need parallel theoretical calculations to make a definite assignment of the observed diffraction pattern, mobility or ionization potential to a specific isomer geometry.

A large amount of theoretical work has been devoted to metallic, semiconductor and noble gas clusters. The work on ionic materials has been centered mostly in the family of alkali halides, and studies of metal oxide clusters have been comparatively scarce, despite their importance in many branches of surface physics, like heterogeneous catalysis or corrosion. Saunders^{9,10} reported mass spectra and collision induced fragmentation data for stoichiometric $(\text{MgO})_n^+$ and $(\text{CaO})_n^+$ cluster ions, Martin and Bergmann¹¹ published mass spectra of $(\text{CaO})_n\text{Ca}^{2+}$ cluster ions, and Ziemann and Castleman¹²⁻¹⁵ performed experimental measurements of several singly- and doubly-ionized cluster ions of MgO and CaO by using laser-ionization time-of-flight mass spectrometry. Theoretical calculations have been performed at different levels of accuracy: simple ionic models based on phenomenological pair potentials were used by Ziemann and Castleman^{13,14} to explain the global trends found in their experiments; Wilson¹⁶ has studied neutral $(\text{MgO})_n$ ($n \leq 30$) clusters by using a compressible-ion model¹⁷ that includes coordination-dependent oxide polarizabilities;^{18,19} semiempirical tight-binding calculations for MgO clusters were reported by Moukouri and Noguera;^{20,21} finally, *ab initio* calculations on stoichiometric MgO clusters have been presented recently by Recio *et al.*,^{22,23} Malliavin and Coudray,²⁴ Li *et al.*,²⁵ and de la Puente *et al.*,²⁶ and calculations on stoichiometric $(\text{Li}_2\text{O})_n$ clusters have been reported by Finocchi and Noguera.²⁷ Regarding the nonstoichiometric cluster ions, Aguado *et al.*²⁸ have studied the structures and stabilities of $(\text{MgO})_n\text{Mg}^{2+}$.

Trying to find an interpretation of the obtained mass spectra, Ziemann and Castleman¹⁴ performed some simple pair potential calculations of the structures of $(\text{MgO})_n\text{Mg}^{2+}$ cluster ions by using a rigid ion model.

The conclusion of those calculations was that the magic numbers can be explained in terms of highly compact structures that can only be obtained for certain cluster sizes, an interpretation very similar to that found in the closely related case of alkali halides.^{29–31} In our previous work,²⁸ we showed that the structures of $(\text{MgO})_n\text{Mg}^{2+}$ cluster ions were quite different from those of alkali halides. Specifically, the influence of the large and coordination dependent polarizabilities of oxide anions (not included in the rigid ion model) favors the formation of surface oxide sites, and thus structures with bulk oxide anions (coordination 6) are not energetically competitive until large values of the number of molecules n are attained. For example, a highly compact $3\times 3\times 3$ cube (where the notation denotes the number of atoms along three perpendicular edges) is not the ground state of $(\text{MgO})_{13}\text{Mg}^{2+}$. Nevertheless, the agreement between the magic numbers obtained through an examination of the stabilities of the clusters against the loss of an MgO molecule and the experimental ones is complete. It is just the interpretation of them in terms of structures that is different, that is, model-dependent. It is interesting to study a similar system like calcium oxide in order to assess whether those trends are a general feature of alkaline-earth oxide clusters or not. Moreover, the experiments of Saunders^{9,10} suggest interesting structural differences between both materials, as the main fragments observed after collisions with inert gas ions were $(\text{MgO})_3$ in one case and $(\text{CaO})_2$ in the other, and the mass spectra of Ziemann and Castleman^{14,15} show different stabilities in the small size regime (magic numbers at $n=5,8,11$ for $(\text{MgO})_n\text{Mg}^{2+}$ and at $n=5,7,9,11$ for $(\text{CaO})_n\text{Ca}^{2+}$), providing further motivation for our study. From the theoretical point of view, Ca^{2+} is larger than Mg^{2+} , so we can expect ionic size packing effects to play an important role in determining structural differences. Besides, Ca^{2+} has a polarizability approximately 6 times larger than Mg^{2+} , and the polarizabilities of the oxide anions are also larger in CaO because the bonding is weaker than in MgO .

In this work we present the results of an extensive and systematic study of $(\text{CaO})_n\text{Ca}^{2+}$ cluster ions with n up to 29, and of $(\text{MgO})_n$ and $(\text{CaO})_n$ neutral stoichiometric clusters with $n=3,6,9,12,15,18$. The rest of the paper is organized as follows: in Section II we give a brief resume of the theoretical model employed, as full an exposition has been reported already in previous works.²⁹ The results are presented in Section III, and the main conclusions to be extracted from our study in Section IV.

II. THE AIPI MODEL AND POLARIZATION CORRECTIONS

The theoretical foundation of the *ab initio* perturbed ion model³² lies in the theory of electronic separability,^{33,34} and its practical implementation in the Hartree-Fock (HF) version of the theory of electronic separability.^{35,36} Very briefly, the HF equations of the

cluster are solved stepwise, by breaking the cluster wave function into local group functions (ionic in nature in our case). In each iteration, the total energy is minimized with respect to variations of the electron density localized in a given ion, with the electron densities of the other ions kept frozen. In the subsequent iterations each frozen ion assumes the role of nonfrozen ion. When the self-consistent process finishes,²⁹ the outputs are the total cluster energy and a set of localized wave functions, one for each geometrically nonequivalent ion of the cluster. These localized cluster-consistent ionic wave functions are then used to estimate the intraatomic correlation energy correction through Clementi's Coulomb-Hartree-Fock method.^{37,38} The large multi-zeta basis sets of Clementi and Roetti³⁹ are used for the description of the ions. At this respect, our optimizations have been performed using basis sets (5s4p) for Mg^{2+} and (5s5p) for O^{2-} , respectively. Inclusion of diffuse basis functions has been checked and shown unnecessary. One important advantage coming from the localized nature of the model is the linear scaling of the computational effort with the number of atoms in the cluster. This has allowed us to study clusters with as many as 59 atoms at a reasonable computational cost.

In our previous work on alkaline-earth oxide clusters,²⁸ we concluded that the aiPI model is equivalent to a first-principles version of the semiempirical breathing shell model.⁴⁰ The binding energy of the cluster can be written as a sum of deformation and interaction terms

$$E_{bind} = \sum_R E_{bind}^R = \sum_R (E_{def}^R + \frac{1}{2}E_{int}^R). \quad (1)$$

where the sum runs over all ions in the cluster. The interaction energy term is of the form

$$E_{int}^R = \sum_{S \neq R} E_{int}^{RS} = \sum_{S \neq R} (E_{class}^{RS} + E_{nc}^{RS} + E_X^{RS} + E_{overlap}^{RS}), \quad (2)$$

where the different energy contributions are: the classical electrostatic interaction energy between point-like ions; the correction to this energy due to the finite extension of the ionic wave functions; the exchange interaction energy between the electrons of ion R and those of the other ions in the cluster; and the overlap repulsive energy contribution.³⁴ The deformation energy term E_{def}^R is the self-energy of the ion R . It is an intrinsically quantum-mechanical many-body term that accounts for the energy change associated to the compression of the ionic wave functions upon cluster formation, and incorporates the correlation contribution to the binding energy. As the model assumes, for computational simplicity, that the ion densities have spherical symmetry, the only relevant terms that are lacking from the *ab initio* description are the polarization terms. In a polarizable point-ion approximation, the polarization contribution to the deformation and interaction energies is

$$E_{int}^{RS,pol} = -\frac{q_R(\vec{\mu}_S\vec{r}_{RS})}{r_{RS}^3} - \frac{q_S(\vec{\mu}_R\vec{r}_{RS})}{r_{RS}^3} - 3\frac{(\vec{\mu}_R\vec{r}_{RS})(\vec{\mu}_S\vec{r}_{RS})}{r_{RS}^5} + \frac{(\vec{\mu}_R\vec{\mu}_S)}{r_{RS}^3}, \quad (3)$$

$$E_{def}^{R,pol} = \frac{\mu_R^2}{2\alpha_R}, \quad (4)$$

where α_R is the polarizability of the ion R, and $\vec{\mu}_R$ the dipole moment induced on ion R. The new terms added to the interaction energy are the monopole-dipole and dipole-dipole interaction energy terms. The term added to the deformation energy represents the energy cost of deforming the charge density of the ion to create the dipole moment. The point-ion approximation provides just the asymptotic part of the polarization interaction energy, that is, it is exact only for large ionic separations. As soon as the ions begin to overlap, there is an important short-range contribution to the induced dipole moments,^{41–45} which is of opposite sign to the asymptotic limit for anions and may in some specific cases reverse the sign of the asymptotic value. These effects can be easily acomodated in the formalism by substituting the asymptotic value of the induced dipole moments by the following expression:

$$\mu_\alpha^{total,R} = \mu_\alpha^{asympt,R} + \mu_\alpha^{sr,R}, \quad (5)$$

with

$$\mu_\alpha^{asympt,R} = \alpha^R \sum_{S \neq R} \frac{r_{RS,\alpha}}{r_{RS}^3} q^R, \quad (6)$$

$$\mu_\alpha^{sr,R} = \alpha^R \sum_{S \neq R} \frac{r_{RS,\alpha}}{r_{RS}^3} f(r_{RS}), \quad (7)$$

where *sr* stands for “short-range” and $\mu_\alpha^{total,R}$ is the α component of the dipole moment vector induced on ion R. The physics behind the short-range polarization correction has been explained in Ref. 41,42, and is associated to the finite extents of the electron densities of the anions and cations. Then, *f* is a short-range function that switches on as the cation-anion overlap becomes appreciable. Madden and coworkers⁴⁵ have employed the Tang and Toennies dispersion damping function⁴⁶ as a suitable form for *f*:

$$f(r_{RS}) = -c \sum_{k=0}^{k_{max}} \frac{b^k}{k!} e^{-br_{RS}}. \quad (8)$$

This is a smoothed step function passing from zero for large *r* to $-c$ for $r=0$. The range of *r* values at which *f* becomes significantly different from zero is primarily determined by the range parameter *b*.

We have included the polarization terms in the energy calculation with this parameterised method, that

calculates the induced dipole moments from eq. (5) and the correction to the deformation and interaction energies from eqs. (3) and (4), respectively. The “enlarged” aiPI+polarization model thus obtained accounts for all the relevant physical interactions. The relaxation of the assumption of spherical symmetry being computationally expensive, the price to be paid is the inclusion in the model of a set of parameters, namely, the polarizabilities α_R and the range parameter *b*. Appropriate values for the other two constants *c* and k_{max} can be taken equal to the bulk values ($c=-3$ and $k_{max}=4$).⁴⁵ Given the meaning of the range parameter *b*, inversely related to half the interionic distance between first neighbors, one might expect different values of *b* for clusters as compared to bulk materials if the interionic distances are substantially different. As a matter of fact, the evolution of those distances with cluster size is not too complicated in the case of ionic clusters.^{26,29–31} Specifically, the average interionic distance *d* initially increases quite abruptly with the number of molecules *n*, and then slowly approaches the bulk limit. As a consequence of this behaviour, we will see that the bulk value ($b=0.75$ a.u.)⁴⁵ is appropriate for all $(CaO)_nCa^{2+}$ clusters with $n \geq 4$. Different values of *b* are needed just for $n < 4$ to avoid overpolarization problems.¹⁶ Regarding the polarizabilities, oxide anions have the interesting property of showing strongly coordination-dependent values. In fact, the O^{2-} anion does not exist as a free ion, which is equivalent to an infinite polarizability; in the solid phase it is stabilized by the crystal environment and has a finite material-dependent polarizability. Wilson¹⁶ has interpolated between those two limits and gives values for the coordination-dependent values of $\alpha(O^{2-})$ in MgO. We have assumed that the ratio of the bulk oxide polarizabilities for MgO and CaO ($\alpha^{bulk}(O^{2-} : CaO)/\alpha^{bulk}(O^{2-} : MgO)=1.469$)⁴⁵ is independent of the oxide coordination, and have deduced the α values for CaO from those of MgO. This procedure is justified because the cation size does not change appreciably with coordination number. For the calcium cation we take the bulk polarizability (3.193 a.u.)⁴⁷

We close this section with a consideration of several criticisms that could be raised against (and of the advantages of) the employed methodology. We have chosen a mixed *ab initio*/semiempirical energy model in order to obtain a good compromise between computational efficiency and accuracy. All the relevant energy terms excluding polarization are described with an *ab initio* methodology. To include polarization, we have used an accurate model,⁴⁵ where the parameters have been fitted by a comparison to *ab initio* calculations.¹⁹ Special care has been devoted to the separation of all the independent physical factors that influence a given quantity, thus avoiding a mixing of different effects in a single parameter and enhancing the transferability of the model. The good parameterisation is reflected in the fact that parameters can be transferred between closely related systems (like, for example, different metal oxides) by simple scaling ar-

guments involving ionic radii.⁴⁸ Thus, we think that the reliability of our calculations is reduced just a little compared to full *ab initio* methodologies. To support this expectation, we made a comparison with DMOL calculations performed on neutral $(\text{CaO})_n$ clusters by Mallavin and Coudray.²⁴ All the interionic distances were in agreement to their calculations up to differences of 4 %. The energetic ordering of the isomers, as well as the specific energy differences, are reproduced with a maximum error of 5 %. We believe that this is a very reasonable agreement, even more if we realize that we are neglecting dispersion interactions, and polarization interactions beyond the dipolar terms. The solid MgO is excellently described with the aiPI model (at least in its static properties).⁴⁹ The model is then expected to transfer properly between both limits. The larger computational simplicity has been exploited to study large cluster sizes (up to 59 ions) with full relaxations of the geometries. Moreover, for each cluster size, a large number of isomers (between 10 and 15) have been investigated. The generation of the initial cluster geometries was accomplished by using a pair potential, as we explained in our previous publication.²⁸ The optimization of the geometries has been performed by using a downhill simplex algorithm.^{50,51}

III. RESULTS AND DISCUSSION

A. Structural Trends in $(\text{CaO})_n\text{Ca}^{2+}$ Cluster Ions

In Fig.1 we present the optimized aiPI+polarization structures of the ground state (GS) and lowest lying isomers or $(\text{CaO})_n\text{Ca}^{2+}$ ($n=4-29$) cluster ions. Below each isomer we show the energy difference (in eV) with respect to the ground state. For $n<4$, the clusters are not detected in the experiments, probably because they undergo a Coulomb explosion driven by the excess charge and the small cluster size, but we are not interested here in this aspect of the experiments. From $n=4$ to $n=10$, there is a predominance of $m\times 2\times 2$ fragments ($m=2-5$), that is, the $(\text{CaO})_2$ subunit appears as the basic building block. The total number of ions in these nonstoichiometric clusters is an odd number, and thus those structures are never perfectly compact. There is either an extra cation added to or a missing anion removed from the perfect structure. Less compact structures as for example planar fragments are not energetically competitive. The structures in this size range tend to be elongated as a direct consequence of the excess cluster charge. When $n=9$, a $3\times 3\times 2+1$ fragment is more stable than that based on the $(\text{CaO})_2$ building block, and $n=10$ is the largest cluster size for which a fragment of this kind is the ground state. Another thing to be pointed out is that in this size range, the extra cation present in the $m\times 2\times 2+1$ structures induces a larger cluster distortion than the missing anion in the $m\times 2\times 2-1$ structures. We will see that this

feature has important implications in the stability of the clusters.

From $n=11$ to $n=15$, the dominant fragments are based on $m\times 3\times 2$ units. For $n=16$ and 17, the most stable isomers are $m\times 4\times 2$ fragments. None of these structures has still developed an anion with full bulk coordination. In particular, the $3\times 3\times 3$ isomer for $n=13$, which is particularly stable in the case of nonstoichiometric alkali halide cluster ions,³¹ does not even appear in Fig. 1. The large coordination-dependent values of the polarizabilities of the oxide anions favors the formation of surface sites, and gives rise to somewhat less compact ground state structures, for which the increase in dipolar energy compensates for the decrease in Madelung energy. The $3\times 3\times 3$ $(\text{CaO})_{13}\text{Ca}^{2+}$ is specially disfavored by the dipolar energy terms because it has a central oxide anion with bulk coordination (so with a comparatively low polarizability), and another 12 anions with coordination 4. On the contrary, the largest coordination in the GS structure is five, and some three-coordinated anions (in corner positions) also appear, inducing a large dipolar energy stabilization. For $n=18$ and 19 there is a glimpse of a transition to more compact cluster structures. The important feature of the GS structures of these two cluster sizes, compared to the $3\times 3\times 3$ for $n=13$, is that now there are oxide anions in corner positions. These make a large contribution to the polarization energy term, that added to the increased Madelung energy of a compact fragment, gives a total GS energy more negative than that of $m\times 3\times 2$ or $m\times 4\times 2$ structures. Nevertheless, the energy differences between isomers are small, and from $n=20$ on, ground state isomers without bulk anions are again obtained ($n=24$ and 27 are the only relevant exceptions, because the ground states of $n=26$ and $n=29$ can be considered degenerate within the accuracy of our theoretical model).

A general feature of $(\text{CaO})_n\text{Ca}^{2+}$ cluster ions with $n\geq 8$ is that $a\times b\times c+1$ fragments are specially stable compared to other isomers whenever they can be formed. In Table I we show all the fragments of that kind relevant to the cluster size range considered in this study. Each series has a typical periodicity that could in principle be reflected in different portions of the mass spectra, given the high stability of these fragments. Some sizes can be accommodated in several families, that is, the classification is highly redundant, but useful anyway to our purposes. If for a given cluster size, a cluster with that formula can be formed, it is always the ground state structure. If it is possible to build up two different isomers with that formula ($n=12, 18, 24$), the more compact structure is energetically favored. This rule works as long as we do not consider structures that are not energetically competitive anymore (the isomer based on the $(\text{CaO})_2$ building block of $(\text{CaO})_{14}\text{Ca}^{2+}$ is an example), and can be helpful in guessing specially stable structures for clusters larger than those studied here. For nearly all those cluster sizes with no competitive $a\times b\times c+1$ structure, $a\times b\times c-1$ fragments are obtained as the ground state or specially stable isomers (examples are found for $n=5, 7, 11, 19, 23$ and

29). The special stability of $a \times b \times c + 1$ structures is sometimes reflected in high stabilities for the corresponding $a \times b \times c + 3$ structures, comparable indeed to the stabilities of $a \times b \times c - 1$ fragments; this occurs for $n=13, 17, 19$ and 26 . With the only exceptions of $n=13, 14, 22, 26$ and 29 , all $(\text{CaO})_n \text{Ca}^{2+}$ GS structures are explained in terms of those three kinds of fragments.

Comparing to the results of our previous paper on $(\text{MgO})_n \text{Mg}^{2+}$ cluster ions,²⁸ we can see that from $n=4$ to $n=20$ the GS structures are basically the same in both systems (the only exceptions are $n=7$ and $n=13$). Interesting structural differences between both materials appear in the size range $n > 20$. Specifically, the transition to bulklike structures, containing inner anions with bulk coordination, is slower in the case of $(\text{CaO})_n \text{Ca}^{2+}$. An analysis of the several energy components shows that the net effect of polarization is more important in calcium oxide. Although the polarizability of Ca^{2+} is larger than that of Mg^{2+} and the coordination-dependent values of $\alpha(\text{O}^{2-})$ are larger in CaO than in MgO, this is not a trivial conclusion, because the interatomic distances are also larger in CaO, and so the electric fields acting on each ion are correspondingly smaller. If we consider that a highly ionic material is that one for which the Madelung energy term is almost completely dominant in determining structural and several other properties, we would conclude that the ionic character of $(\text{CaO})_n \text{Ca}^{2+}$ is smaller than that found for $(\text{MgO})_n \text{Mg}^{2+}$. Indeed, being the polarization contribution more important, the structures of calcium oxide clusters have a larger directionality degree, a feature that is usually associated to covalency (opposite to the natural tendency of purely ionic systems to form isotropic structures). However, we think that the term “covalency” should be employed just in those situations where charge transfer between different atomic centers is important. As Madden and coworkers have discussed,⁴³ polarization terms in ionic systems are responsible for a lot of properties traditionally attributed to “covalency”. One point that deserves further investigation, however, is whether the directional properties induced by polarization effects (and reflected in a lower average coordination) can be responsible for a larger charge transfer between different centers. This would be reasonable because the saturation of the bonds is less complete.

B. Relative stabilities and connection to experimental mass spectra

In the experimental mass spectra,^{11,15} the populations observed for some cluster sizes are enhanced over those of the neighboring sizes. These “magic numbers” are a consequence of the evaporation events that occur in the cluster beam, mostly after ionization.⁵² A magic cluster of size n has an evaporation energy that is large compared to that of the neighboring sizes $(n-1)$ and $(n+1)$. Thus, on the average, clusters of size n undergo a smaller number of evaporation events and this leads to the maxima

in the mass spectra. As our main concern in this section is to compare with the experimental mass spectra, we calculate the evaporation energy as a function of cluster size. To do this, we assume that the dominant evaporation channel is the loss of a neutral (CaO) molecule, something supported by the experiments of Ziemann and Castleman.¹⁵ In the size range $n < 11$, some other channels seem to be opened in the experiments,¹⁵ and indeed for $n < 4$ Coulomb explosion is dominant, that is the reason why we do not consider clusters with $n < 4$. With that assumption, the evaporation energy of $(\text{CaO})_n \text{Ca}^{2+}$ reads

$$E_{\text{evap}}(n) = E_{\text{cluster}}[(\text{CaO})_{n-1} \text{Ca}^{2+}] + E(\text{CaO}) - E_{\text{cluster}}[(\text{CaO})_n \text{Ca}^{2+}]. \quad (9)$$

Maxima in the evaporation energy curve do not always coincide with maxima in the experimental mass spectra.²⁸ There are two main processes that contribute to enhance the cluster population for size n : a) A small evaporation energy for size $(n+1)$; b) A large evaporation energy for size n . Thus, a most convenient quantity to compare with experiment is the second energy difference

$$\Delta_2(n) = E_{\text{evap}}(n+1) - E_{\text{evap}}(n). \quad (10)$$

A negative value of $\Delta_2(n)$ indicates that the n -population increases by evaporations from the $(n+1)$ -clusters more rapidly than it decays by evaporation to the $(n-1)$ -clusters. Specifically, the specially stable cluster sizes will be reflected as minima in the $\Delta_2(n)$ curve.

Now, the evaporation energy $E_{\text{evap}}(n)$ of eq. (9) can be calculated in two different ways. In the first one, energy differences are always taken between the ground state structures of sizes n and $(n-1)$. This procedure, which we call (by obvious reasons) adiabatic evaporation, reflects the stability of the clusters in the limit of small energy barriers between isomers or alternatively of large experimental times of flight. The stabilities calculated in this way are shown in the upper part of figure 2. Magic numbers are found for $n=5, 8, 12, 15, 18, 20, 24, 27$. The only $a \times b \times c - 1$ structure that shows a special stability is that of $n=5$. The rest of magic clusters belong to the $a \times b \times c + 1$ family of structures. If n is a magic size, and both $(n+1)$ and $(n-1)$ GS structures do not belong to the $a \times b \times c + 1$ family, a deep minima is found in the $\Delta_2(n)$ curve (this happens for $n=12$ and 18). For the rest of magic sizes, the $(n+1)$ GS structure has also the formula $a \times b \times c + 1$, and has a correspondingly high stability reflected in a negative value of $\Delta_2(n+1)$. In these cases the stability of size n is just slightly enhanced over that of size $(n+1)$. One can appreciate the increasing relevance of the Madelung term in determining the cluster stabilities: when $n < 20$, the most stable $a \times b \times c + 1$ structures are the less compact ones ($n=8$ and 15 more stable than $n=9$ and 16 , respectively); if $n \geq 20$, that trend is reversed ($n=20, 24$ and 27 more stable than $n=21, 25$, and 28 , respectively). The special relevance of $a \times b \times c + 1$ structures in explaining the cluster stabilities does not

conform to the initial experimental expectations of high stabilities for $a \times b \times c - 1$ structures.¹⁵ Analysing the energy components, we find that the polarization contribution stabilizes the $a \times b \times c + 1$ structure more than the corresponding $a \times b \times c - 1$ structure for all values of a, b, c . For the smallest cluster sizes, however, the extra cation present in $a \times b \times c + 1$ structures induces a large cluster distortion compared to that induced by the missing anion in $a \times b \times c - 1$ structures, and the Madelung contribution favors these last structures in a larger amount, making them more stable for some sizes.

The second kind of calculation of $E_{evap}(n)$ proceeds as follows: we consider the optimized GS structure of $(\text{CaO})_n \text{Ca}^{2+}$ and identify the CaO molecule that contributes the least to the cluster binding energy. Then we remove that molecule and relax the resulting $(\text{CaO})_{n-1} \text{Ca}^{2+}$ fragment to the nearest local minimum. This process can be termed locally adiabatic because both fragments are allowed to relax to the local minimum energy configuration after the evaporation. For some cluster sizes, the fragment of size $(n-1)$ left when a CaO molecule is removed from $(\text{CaO})_n \text{Ca}^{2+}$ does not lie on the catchment basin of the $(\text{CaO})_{n-1} \text{Ca}^{2+}$ GS isomer, so that the locally adiabatic evaporation energies are larger than the energy differences between adjacent ground states minus $E(\text{CaO})$ in those cases. The locally adiabatic evaporation energies are plotted as a function of n in the lower part of Fig. 2. These will reflect the cluster stabilities in the limit of large energy barriers between isomers or of short experimental times of flight. Magic numbers are obtained for $n=5,7,9,11,13,16,19,22,25$ and 27 , in complete agreement with the experiments of Ziemann and Castleman.¹⁵

The main message to be extracted from these considerations is that the magic numbers obtained in the experiments might be dominated by the effects of kinetic traps occurring in the course of the evaporation process. Since our calculations are static, we can not rigorously assert that this is the only possible explanation, but a plausibility argument based on a comparison to the closely related and more thoroughly studied case of alkali halides supports our expectations. The mobility experiments performed by the group of Jarrold^{5,6} show that the relaxation dynamics to the ground state structure for sodium chloride clusters involves drift times of almost one second. The importance of kinetic traps in explaining these interesting results is shown in the theoretical works of Doye and Wales.⁵³ Specifically, these authors show that the potential energy landscape of alkali halide clusters, calculated by using a phenomenological pair potential to describe the interactions, is structured in several funnels, separated from each other by high free-energy barriers. When a cluster evaporates a molecule, it cools in the process, so trapping kinetic effects are expected whenever parent and product GS structures belong to different funnels. Given the close similarities between halide and oxide systems, one expects similar effects in the evaporation kinetics of alkaline-earth oxides to be relevant.

The main structural differences are due to the effects of polarization, and these could also affect the mechanisms of structural transitions. In the case of alkali halides, Doye and Wales find that a highly cooperative process is energetically less impeded by energy barriers than sequential ionic diffusion,⁵³ with interesting implications for the mechanical properties of these clusters. Perhaps the same is true for the clusters studied here, but one has to keep in mind that polarization tends to lower the barriers against diffusion,⁵⁴ and those effects are more important for oxides. We think that further calculations of this kind for oxide clusters would be very interesting. Mobility experiments on $(\text{MgO})_n \text{Mg}^{2+}$ or $(\text{CaO})_n \text{Ca}^{2+}$ could conclusively confirm the structural trends found in the present work.

C. Neutral Stoichiometric $(\text{MgO})_n$ and $(\text{CaO})_n$ clusters

The experiments performed by Saunders^{9,10} show that both $(\text{MgO})_n^+$ and $(\text{CaO})_n^+$ stoichiometric cluster ions with a number of molecules $n=6,9,12$ and 15 are especially abundant in the mass spectra. However, when these clusters are allowed to collide with inert gas ions, the fragmentation channels are different: $(\text{MgO})_3$ fragments are predominantly observed in one case and $(\text{CaO})_2$ fragments in the other. These results suggest that the basic cluster building blocks are different for the two materials, but not so different as to lead to different magic numbers.

We found a similar scenario in the case of alkali halide clusters.³⁰ Specifically, a universal set of magic numbers $n=4,6,9,12,\dots$ was found for the whole family of $(\text{AX})_n$ clusters, with $A=\text{Li,Na,K,Rb}$ and $X=\text{F,Cl,Br,I}$. However, the cluster structures were not found to be the same for all the different materials. When the cation size is much smaller than the anion size (all lithium halides and sodium iodide),²⁹ ground state structures based on the stacking of hexagonal $(\text{AX})_3$ rings are obtained. For the rest of materials, the ground state structures are mostly obtained by stacking of rectangular (or double-chain) $(\text{AX})_3$ planar fragments. This is just a packing effect: when the ratio of cation to anion size is very small, anion-anion overlap repulsive interactions are large, forcing an opening of the $(\text{AX})_3$ rectangular fragments into hexagons. The magic numbers are the same for both structural families because it is for those cluster sizes that specially compact structures can be formed. When we studied $(\text{AX})_n \text{A}^+$ alkali halide cluster ions,³¹ we found that the structures were much more similar irrespective of packing considerations. The ring structures are not competitive in this case because it is not possible to build up a perfect hexagonal fragment with an odd number of ions. On the contrary, perfect cubic structures can be formed (as for example the $3 \times 3 \times 3$ structure for $n=13$).

From our study on doubly-charged clusters, we have not found important structural differences between

$(\text{CaO})_n\text{Ca}^{2+}$ and $(\text{MgO})_n\text{Mg}^{2+}$,²⁸ at least in the small size regime. We have performed aiPI+polarization calculations on the structures of $(\text{MgO})_n$ and $(\text{CaO})_n$ with $n=3,6,9,12,15$ and 18. Specifically, we have considered just those structures based on staking of hexagonal and rectangular $(\text{AO})_3$ units, and those based on stacking of $(\text{AO})_2$ units, with $A=\text{Mg}$ or Ca . We find that the ground state structures of $(\text{MgO})_n$ clusters are based on $(\text{MgO})_3$ units, while those of $(\text{CaO})_n$ clusters have a rectangular $(\text{CaO})_3$ building block, being this the same packing effect found in the case of alkali halides. The structure of $(\text{CaO})_6$ could be alternatively viewed as the stacking of three $(\text{CaO})_2$ units, but for $n=9,12,15$ and 18, the tubular shapes obtained by stacking $(\text{CaO})_2$ units are not competitive anymore. Were all the ground state structures of $(\text{CaO})_n$ clusters based on the $(\text{CaO})_2$ building block, we would expect a periodicity of 2 in the magic numbers observed in the mass spectra. Saunders shows the collision induced fragmentation spectra of $(\text{CaO})_n$, with $n=4,6,8$,⁹ which are certainly based on stacking of $(\text{CaO})_2$ units, but does not show those for $(\text{CaO})_9$ or $(\text{CaO})_{12}$, for example. Our main conclusion is that the special stability of $(\text{CaO})_n$ clusters is also explained in terms of $(\text{CaO})_3$ units, but with rectangular instead of hexagonal shape. This explains the same periodicities observed in the magic numbers of both materials.

IV. SUMMARY

The *ab initio* perturbed ion model, supplemented with a parameterised treatment of dipolar terms, has been employed in order to study the structural and energetic properties of $(\text{CaO})_n\text{Ca}^{2+}$ ($n=1-29$) cluster ions. Polarization effects favor the formation of surface sites, and reduce the stability of highly compact structures containing anions with bulk coordination. Thus, despite many similarities in the experimental mass spectra, the structures of alkaline-earth oxide and alkali halide cluster ions are shown to be different. Most of the lowest energy structures have the formula $a \times b \times c + 1$. The structures of $(\text{CaO})_n\text{Ca}^{2+}$ and $(\text{MgO})_n\text{Mg}^{2+}$ cluster ions are very similar for $n < 20$, irrespective of differences in cationic size and polarization. It is just for $n \geq 20$ that structural differences emerge, showing a slower convergence to bulk properties for CaO compared to MgO . The analysis of the stabilities suggests that the experimental mass spectra could be dominated by the effects of kinetic traps. Specifically, if we consider locally adiabatic evaporation events, complete agreement is found with the experimental stabilities. The neutral stoichiometric $(\text{MgO})_n$ and $(\text{CaO})_n$ clusters ($n=3,6,9,12,15,18$) show structural differences similar to those observed in neutral stoichiometric alkali halide clusters: the basic building block is an $(\text{MgO})_3$ hexagonal fragment in the case of MgO and a $(\text{CaO})_3$ rectangular (or double-chain) fragment in the case of CaO . This is just a packing effect due to the

larger overlap repulsion between anions when the cation size is very small. While the structures of $(\text{CaO})_n$ clusters, with $n=4,6,8$ are certainly based on $(\text{CaO})_2$ units, as suggested by collision-induced fragmentation experiments, the specially stable $(\text{CaO})_n$ clusters are based on a $(\text{CaO})_3$ unit. This explains the same periodicity of 3 observed in the experimental magic numbers of both $(\text{MgO})_3^+$ and $(\text{CaO})_3^+$ clusters.

Captions of Figures and Tables.

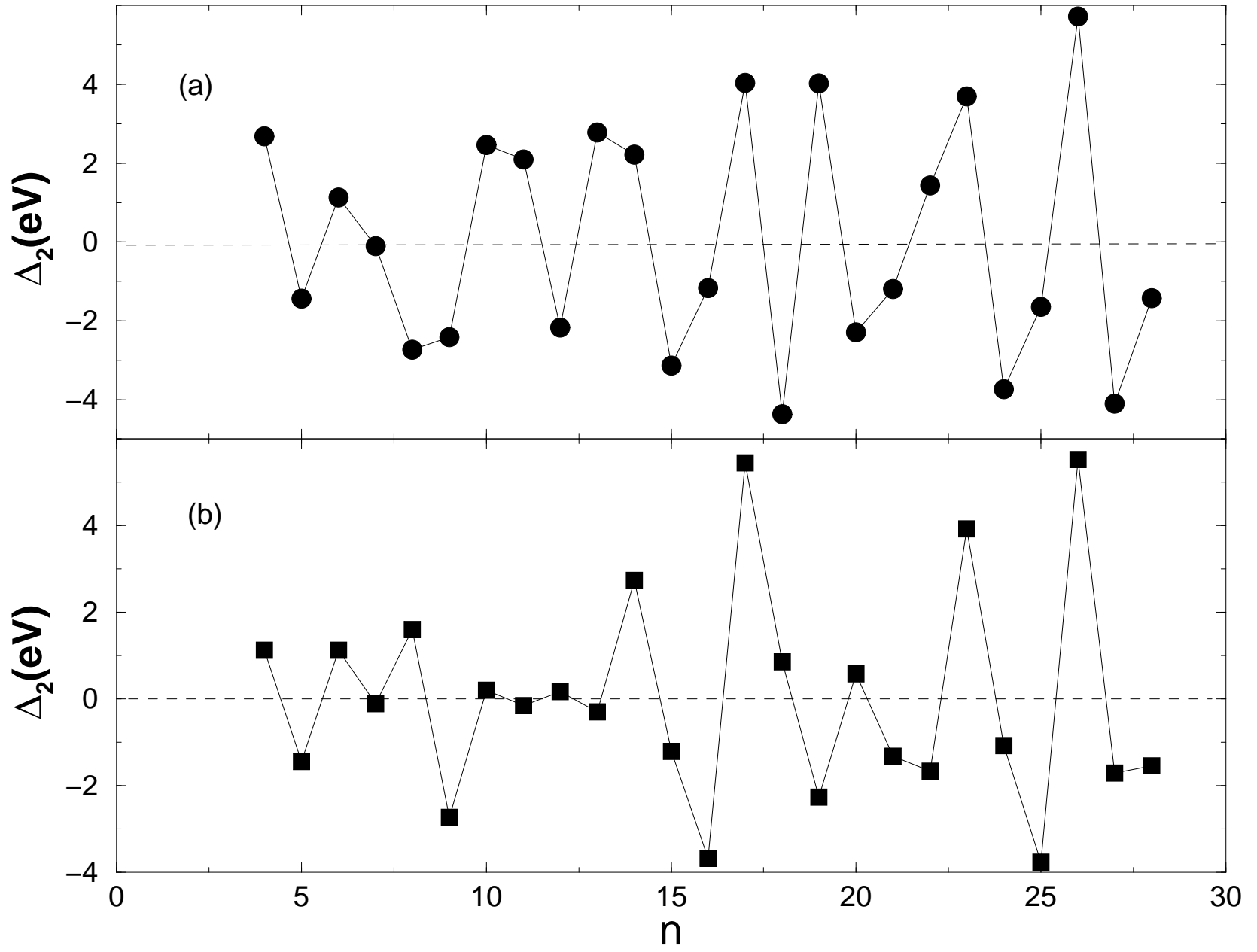
Figure 1. Lowest-energy structure and low-lying isomers of $(\text{CaO})_n\text{Ca}^{2+}$ cluster ions. Dark balls are Ca^{2+} cations and light balls are O^{2-} anions. The energy difference (in eV) with respect to the most stable structure is given below the corresponding isomers.

Figure 2. Adiabatic (a) and locally adiabatic (b) evaporation energies required to remove a neutral CaO molecule from $(\text{CaO})_n\text{Ca}^{2+}$ cluster ions as a function of n . The local minima in the evaporation energy curve are shown explicitly.

Table I Possible different $a \times b \times c + 1$ structures, with their inherent periodicities. Those cluster sizes n that are actually observed as ground state structures of $(\text{CaO})_n\text{Ca}^{2+}$ clusters are written in boldface.

Structure	Periodicity	Cluster size n
$m \times 2 \times 2 + 1$	2	8,10,12 ,...
$m \times 3 \times 2 + 1$	3	9,12,15,18,21,24,27 ...
$m \times 4 \times 2 + 1$	4	8,12,16,20,24,28 ,...
$m \times 5 \times 2 + 1$	5	10,15,20,25 ,...
$m \times 6 \times 2 + 1$	6	12,18,24,...
$m \times 3 \times 3 + 1$	9	9,18,27 ,...
$m \times 4 \times 3 + 1$	6	12,18,24 ,...

-
- ¹ Maier-Borst, M.; Cameron, D. B.; Rokni, M.; Parks, J. H.; *Phys. Rev. A* **1999**, *59*, R3162
- ² von Helden, G.; Hsu, M. T.; Kemper, P. R.; Bowers, M. T.; *J. Chem. Phys.* **1991**, *95*, 3835
- ³ Jarrold, M. F.; *J. Phys. Chem.* **1995**, *99*, 11
- ⁴ Maier-Borst, M.; Löffler, P.; Petry, J.; Kreisle, D.; *Z. Phys. D* **1997**, *40*, 476; Löffler, P.; Lilienthal, A.; Kreisle, D.; private communication.
- ⁵ Dugourd, P.; Hudgins, R. R.; Jarrold, M. F.; *Chem. Phys. Lett.* **1997**, *267*, 186
- ⁶ Hudgins, R. R.; Dugourd, P.; Tenenbaum, J. M.; Jarrold, M. F.; *Phys. Rev. Lett.* **1997**, *78*, 4213
- ⁷ Fatemi, F. K.; Fatemi, D. J.; Bloomfield, L. A.; *Phys. Rev. Lett.* **1996**, *77*, 4895; Fatemi, D. J.; Fatemi, F. K.; Bloomfield, L. A.; *Phys. Rev. A* **1996**, *54*, 3674; Fatemi, F. K.; Fatemi, D. J.; Bloomfield, L. A.; *J. Chem. Phys.* **1999**, *110*, 5100; Fatemi, F. K.; Dally, A. J.; Bloomfield, L. A.; *Phys. Rev. Lett.* **2000**, *84*, 51
- ⁸ Boutou, V.; Lebeault, M. A.; Allouche, A. R.; Bordas, C.; Paulig, F.; Viallon, J.; Chevalerey, J.; *Phys. Rev. Lett.* **1998**, *80*, 2817
- ⁹ Saunders, W. A.; *Phys. Rev. B* **1988**, *37*, 6583
- ¹⁰ Saunders, W. A.; *Z. Phys. D* **1989**, *12*, 601
- ¹¹ Martin, T. P.; Bergmann, T.; *J. Chem. Phys.* **1989**, *90*, 6664
- ¹² Ziemann, P. J.; Castleman, A. W.; *Z. Phys. D* **1991**, *20*, 97
- ¹³ Ziemann, P. J.; Castleman, A. W.; *J. Chem. Phys.* **1991**, *94*, 718
- ¹⁴ Ziemann, P. J.; Castleman, A. W.; *Phys. Rev. B* **1991**, *44*, 6488
- ¹⁵ Ziemann, P. J.; Castleman, A. W.; *J. Phys. Chem.* **1992**, *96*, 4271
- ¹⁶ Wilson, M.; *J. Phys. Chem. B* **1997**, *101*, 4917
- ¹⁷ Wilson, M.; Madden, P. A.; Pyper, N. C.; Harding, J. H.; *J. Chem. Phys.* **1996**, *104*, 8068
- ¹⁸ Fowler, P. W.; Tole, P.; *Surf. Sci.* **1988**, *197*, 457
- ¹⁹ Jemmer, P.; Fowler, P. W.; Wilson, M.; Madden, P. A.; *J. Phys. Chem. A* **1998**, *102*, 8377, and references therein.
- ²⁰ Moukouri, S.; Noguera, C.; *Z. Phys. D* **1992**, *24*, 71
- ²¹ Moukouri, S.; Noguera, C.; *Z. Phys. D* **1993**, *27*, 79
- ²² Recio, J. M.; Pandey, R.; *Phys. Rev. A* **1993**, *47*, 2075
- ²³ Recio, J. M.; Pandey, R.; Ayuela, A.; Kunz, A. B.; *J. Chem. Phys.* **1993**, *98*, 4783
- ²⁴ Malliavin, M. J.; Coudray, C.; *J. Chem. Phys.* **1997**, *106*, 2323
- ²⁵ Li, Y.; Langreth, D. C.; Pederson, M. R.; *Phys. Rev. B* **1997**, *55*, 16456
- ²⁶ de la Puente, E.; Aguado, A.; Ayuela, A.; López, J. M.; *Phys. Rev. B* **1997**, *56*, 7607
- ²⁷ Finocchi, F.; Noguera, C.; *Phys. Rev. B* **1996**, *53*, 4989
- ²⁸ Aguado, A.; López-Gejo, F.; López, J. M.; *J. Chem. Phys.* **1999**, *110*, 4788
- ²⁹ Aguado, A.; Ayuela, A.; López, J. M.; Alonso, J. A.; *J. Phys. Chem. B* **1997**, *101*, 5944
- ³⁰ Aguado, A.; Ayuela, A.; López, J. M.; Alonso, J. A.; *Phys. Rev. B* **1997**, *56*, 15353
- ³¹ Aguado, A.; Ayuela, A.; López, J. M.; Alonso, J. A.; *Phys. Rev. B* **1998**, *58*, 9972
- ³² Luaña, V.; Pueyo, L.; *Phys. Rev. B* **1990**, *41*, 3800
- ³³ McWeeny, R.; *Methods of molecular quantum mechanics*; Academic Press; London, 1994
- ³⁴ Francisco, E.; Martín Pendás, A.; Adams, W. H.; *J. Chem. Phys.* **1992**, *97*, 6504
- ³⁵ Huzinaga, S.; Cantu, A. A.; *J. Chem. Phys.* **1971**, *55*, 5543
- ³⁶ Huzinaga, S.; McWilliams, D.; Cantu, A. A.; *Adv. Quantum Chem.* **1973**, *7*, 183
- ³⁷ Clementi, E.; *IBM J. Res. Develop.* **1965**, *9*, 2
- ³⁸ Chakravorty, S. J.; Clementi, E.; *Phys. Rev. A* **1989**, *39*, 2290
- ³⁹ Clementi, E.; Roetti, C.; *At. Data and Nuc. Data Tables* **1974**, *14*, 177
- ⁴⁰ Matsui, M.; *J. Chem. Phys.* **1998**, *108*, 3304
- ⁴¹ Szigeti, B.; *Proc. Roy. Soc. (London)* **1950**, *A204*, 1076
- ⁴² Fowler, P. W.; Madden, P. A.; *Phys. Rev. B* **1984**, *29*, 1035; *ibid.* **1985**, *31*, 5443
- ⁴³ Madden, P. A.; Wilson, M.; *Chem. Soc. Rev.* **1996**, *25*, 399
- ⁴⁴ Rowley, A. J.; Jemmer, P.; Wilson, M.; Madden, P. A.; *J. Chem. Phys.* **1998**, *108*, 10209
- ⁴⁵ Jemmer, P.; Wilson, M.; Madden, P. A.; Fowler, P. W.; *J. Chem. Phys.* **1999**, *111*, 2038
- ⁴⁶ Tang, K. T.; Toennies, J. P.; *J. Chem. Phys.* **1984**, *80*, 3726
- ⁴⁷ Fowler, P. W.; Pyper, N. C.; *Proc. R. Soc. Lond. A* **1985**, *398*, 377
- ⁴⁸ Rowley, A. J.; Wilson, M.; Madden, P. A.; *J. Phys.: Condens. Matter* **1999**, *11*, 1903
- ⁴⁹ Luaña, V.; Recio, J. M.; Pueyo, L.; *Phys. Rev. B* **1990**, *42*, 1791
- ⁵⁰ Nelder, J. A.; Mead, R.; *Comput. J.* **1965**, *7*, 308
- ⁵¹ Press, W. H.; Teukolsky, S. A.; *Computers in Physics* **1991**, *5*, 426
- ⁵² Ens, W.; Beavis, R.; Standing, K. G.; *Phys. Rev. Lett.* **1983**, *50*, 27
- ⁵³ Doye, J. P. K.; Wales, D. J.; *Phys. Rev. B* **1999**, *59*, 2292; *J. Chem. Phys.* **1999**, *111*, 11070
- ⁵⁴ Wilson, N. T.; Wilson, M.; Madden, P. A.; Pyper, N. C.; *J. Chem. Phys.* **1996**, *105*, 11209



This figure "4to8.xfig.gif" is available in "gif" format from:

<http://arxiv.org/ps/physics/0004041v4>

This figure "9to13.xfig.gif" is available in "gif" format from:

<http://arxiv.org/ps/physics/0004041v4>

This figure "14to18.xfig.gif" is available in "gif" format from:

<http://arxiv.org/ps/physics/0004041v4>

This figure "19to23.xfig.gif" is available in "gif" format from:

<http://arxiv.org/ps/physics/0004041v4>

This figure "24to28.xfig.gif" is available in "gif" format from:

<http://arxiv.org/ps/physics/0004041v4>

This figure "29to30.xfig.gif" is available in "gif" format from:

<http://arxiv.org/ps/physics/0004041v4>